PERGAMON

Engineering Fracture Mechanics 68 (2001) 107–125

Engineering Fracture Mechanics

www.elsevier.com/locate/engfracmech

Probabilistic fracture mechanics: *J*-estimation and finite element methods

Sharif Rahman *,[1]

Department of Mechanical Engineering, The University of Iowa, Iowa City, IA 52242, USA

Received 31 August 1998; received in revised form 21 March 2000; accepted 10 August 2000

Abstract

The objective of this study was to evaluate the adequacy of current *J*-estimation models commonly used in probabilistic elastic–plastic analysis of ductile cracked structures. A newly developed probabilistic model based on elastic–plastic finite element method was used to evaluate the *J*-estimation model. In both models, the analyses involve elastic–plastic fracture mechanics for underlying deterministic calculations, statistical representation of uncertainties in loads, crack size, and material properties involving both tensile and fracture toughness characteristics, and standard computational methods of structural reliability theory. Numerical examples are presented for two- and three-dimensional cracked structures. The results show that the probabilistic analysis based on *J*-estimation model provides accurate estimates of failure probability when compared with those predicted by generally more accurate finite element model. The uncertainty in the crack size, if exists, can have a significant effect on the probability of failure, particularly when the crack size has a large coefficient of variation. A finite element-based probabilistic fracture-mechanics model is useful in benchmarking approximate results of *J*-estimation analysis.

Keywords: Probabilistic fracture mechanics; Elastic–plastic fracture mechanics; *J*-integral; Crack; First- and second-order reliability methods; Failure probability; Fracture; *J*-estimation method

1. Introduction

In recent years, probabilistic fracture mechanics (PFM) is becoming increasingly popular for realistic evaluation of fracture response and reliability of cracked structures. Using PFM, one can incorporate statistical uncertainties in engineering design and evaluation – a need, which has long been recognized. The theory of fracture mechanics provides a mechanistic relationship between the maximum permissible load acting on a structural component to the size and location of a crack – either real or postulated – in that component. The theory of probability determines how the uncertainties in crack size, loads, and material properties, if modeled accurately, affect the integrity of cracked structures. PFM, which blends these two

* Tel.: +1-319-335-5679; fax: +1-319-335-5669.
E-mail address: rahman@engineering.uiowa.edu (S. Rahman).
[1] Website: http://www.engineering.uiowa.edu/~rahman.

0013-7944/00/$ - see front matter
PII: S0013-7944(00)00092-8

theories, accounts for both mechanistic and statistical aspects of a fracture problem, and hence, provides a more rational way of describing the actual behavior and reliability of structures than the traditional deterministic models.

The fracture analysis can be based on linear-elastic or more complex elastic–plastic (nonlinear) models. It is now well established that the nonlinear fracture-mechanics methods provide more realistic measures of fracture behavior of cracked structures with high toughness and low strength materials compared with the elastic methods. Cracked components made of these materials in nuclear power plants, chemical and fossil plants, automobiles, and aerospace and aircraft propulsion systems pose a serious threat to structural integrity. In much or all of the working temperature regime of these components, the material is being typically stressed above the brittle-to-ductile transition temperature where the fracture response is essentially ductile and the material is capable of considerable inelastic deformation. As such, elastic–plastic theories should be used for fracture analyses of these structural components. While the development is still ongoing, significant progress has been made in the deterministic modeling of both linear-elastic fracture mechanics (LEFM) and elastic–plastic fracture mechanics (EPFM). Probabilistic models have also been developed to estimate various response statistics and reliability [1]. Currently, there are many applications of PFM in the field of oil and gas, nuclear, automotive, naval, aerospace, and other industries. Nearly all of these methods have been developed strictly based on LEFM models. On the other hand, the probabilistic analysis based on EPFM models has received only a limited attention to date. Probabilistic analyses based on EPFM models are just beginning to appear, particularly, for applications in pressure boundary components [2–8].

In EPFM, the crack-driving force is frequently described in terms of J-integral. The J-integral is an appropriate fracture parameter that describes the crack-tip stress and strain fields adequately when there are no constraint effects. Similar to any deterministic EPFM problem, the evaluation of J-integral for probabilistic analysis can be performed by (1) numerical method and (2) engineering estimation method. Traditionally, a numerical study has been based on elastic–plastic finite element method (FEM). Using FEM, one can calculate J for any crack geometry and load conditions. However, it is also useful to have simplified estimation methods for routine engineering calculations. Accordingly, the probabilistic EPFM analyses based on both methods have been reported. For example, in the US Nuclear Regulatory Commission's Short Cracks in Piping and Piping Welds Program [9], a probabilistic model was developed for elastic–plastic analysis of circumferential through-wall cracks in pipes for leak-before-break applications [6]. This model involves a J-estimation method, statistical representation of uncertainties in loads, crack size, and material properties, and first- and second-order reliability methods (FORM/SORM). Shortly thereafter, similar probabilistic models based on other J-estimation formulas have also been reported [2–5]. In these models, the estimation formulas typically consist of closed-form equations of J as a function of load, crack size, and material properties of a structure and hence, do not require any expensive nonlinear finite element calculations. Actually, this is a major reason why the FORM/SORM algorithms have been successfully developed for probabilistic analysis of elastic–plastic structures [2–6]. However, due to various approximations and/or limitations in the J-estimation method, one needs to evaluate its accuracy by comparing with generally more accurate FEM-based probabilistic analysis. To date, no such evaluations have been conducted or reported. It is worth noting that a probabilistic model based on elastic–plastic FEM has already been developed by some researchers [7,8].

This paper presents the results of comparisons of two probabilistic EPFM models based on J-estimation and FEMs. In both models, the analyses involve (1) EPFM, (2) statistical models of loads, crack size, and material properties including stress–strain and fracture toughness curves, and (3) standard reliability methods. A major objective was to determine if a model based on J-estimation method is adequate for probabilistic EPFM analysis. Two- and three-dimensional examples are presented to conduct the probabilistic analysis.

2. Elastic–plastic fracture mechanics

In order to perform elastic–plastic analysis, the material model needs to be defined. In this study, it was assumed that the constitutive law characterizing the material's stress–strain ($\sigma-\varepsilon$) response can be represented by the well-known Ramberg–Osgood model, which is given by

$$\frac{\varepsilon}{\varepsilon_0} = \frac{\sigma}{\sigma_0} + \alpha \left(\frac{\sigma}{\sigma_0}\right)^n \tag{1}$$

where σ_0 is the reference stress which is usually assumed to be the yield stress, E is the modulus of elasticity, $\varepsilon_0 = \sigma_0/E$ is the associated reference strain, and α and n are the model parameters usually chosen from best fit of actual laboratory data. Although this representation of the stress–strain curve is not necessary for the finite element analysis, it is needed for most, if not all, of the J-estimation methods, which are formulated based on power-law idealization.

The J-integral parameter proposed by Rice [10] is extensively used in assessing fracture integrity of cracked engineering structures, which undergo large plastic deformation at the crack tip. For elastic–plastic problems, its interpretation as the strength of the asymptotic crack-tip fields by Hutchinson [11] and Rice and Rosengren [12] represents the crux of the basis for "J-controlled" crack growth behavior. For a cracked body with an arbitrary counter-clockwise path, Γ around the crack tip (see Fig. 1(a)), a formal definition of J under mode-I condition is

$$J \overset{\text{def}}{=} \int_{\Gamma} (\mathscr{W} n_1 - T_i u_{i,1})\, \mathrm{d}S \tag{2}$$

where, $\mathscr{W} = \int \sigma_{ij}\, \mathrm{d}\varepsilon_{ij}$ is the strain energy density with σ_{ij} and ε_{ij} representing components of stress and strain tensors, respectively, u_i and $T_i = \sigma_{ij} n_j$ are the ith component of displacement and traction vectors, n_j is the jth component of unit outward normal to integration path, $\mathrm{d}S$ is the differential length along contour Γ, and $u_{i,1} = \partial u_i/\partial x_1$ is the differentiation of displacement with respect to x_1. Here, the summation convention is adopted for repeated indices.

The J-integral is theoretically valid for nonlinear elasticity or deformation theory of plasticity where no or little unloading occurs. It is frequently used to characterize initiation of crack growth and a small amount of crack propagation. A wealth of comparisons between predictions based on J-integral versus experimental data now show that fairly accurate results can be obtained for monotonic loading to failure even though the theoretical conditions for a valid J-based fracture theory are violated [13–16]. In this study, the elastic–plastic analyses of cracks will focus only on the J-integral fracture parameter.

2.1. J-integral by finite element method

For numerical calculation of J, the energy domain integral methodology [17,18] was used in the finite element analysis. Using the divergence theorem, the contour integral defined in Eq. (1) can be expanded into an area integral in two dimensions, and volume integral in three-dimensions, over a finite domain surrounding the crack tip or crack front. For a linear or nonlinear elastic material under quasi-static condition, in the absence of body forces, thermal strains, and crack-face tractions, Eq. (1) for two-dimensional problem reduces to

$$J = \int_{A^*} \left[\sigma_{ij} \frac{\partial u_j}{\partial x_1} - \mathscr{W} \delta_{1i}\right] \frac{\partial q}{\partial x_i}\, \mathrm{d}A \tag{3}$$

where δ_{ij} is Kronecker delta, q is an arbitrary but smooth weighting function that is equal to *unity* on Γ_0 and *zero* on Γ_1, and A^* is the annular area enclosed by the inner contour Γ_0 and outer contour Γ_1 as shown

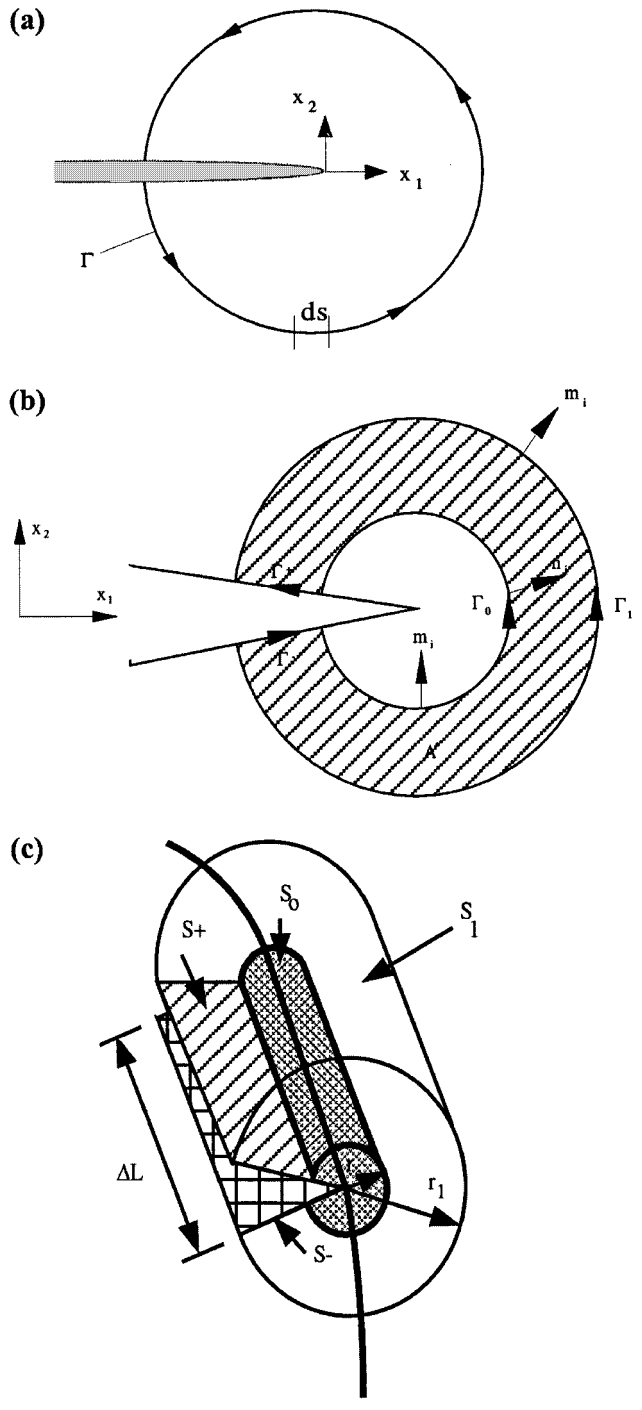

Fig. 1. *J*-integral as an elastic–plastic fracture parameter: (a) arbitrary contour around a crack tip; (b) inner and outer contours enclosing A^* and (c) inner and outer surfaces enclosing V^*.

in Fig. 1(b). For three-dimensional problem, a similar expression of J involving volume integral can be developed and is given by

$$J = \int_{V^*} \left[\sigma_{ij} \frac{\partial u_j}{\partial x_1} - \mathscr{W} \delta_{1i} \right] \frac{\partial q}{\partial x_i} \mathrm{d}V \tag{4}$$

where V^* is the volume enclosed by the inner surface S_0 and outer surface S_1 as shown in Fig. 1(c). The discrete form of these domain integrals is [19]

$$J \cong \sum_{A^* \text{ or } V^*} \sum_{l=1}^{m} \left\{ \left[\left(\sigma_{ij} \frac{\partial u_j}{\partial x_1} - \mathscr{W} \delta_{1i} \right) \frac{\partial q}{\partial x_i} \right] \left| \frac{\partial x_j}{\partial \xi_k} \right| \right\}_l w_l \tag{5}$$

where m is the number of Gauss points per element, ξ_k is the parametric coordinate, and w_l is the weighting factor. Further details on finite element implementation of J are given by Anderson [19].

2.2. J-integral by engineering estimation method

Simple mathematical models, often referred to as the J-estimation methods, are based on assumptions necessary to minimize the need for elaborate numerical analysis (e.g., FEM). Typically, such assumptions lead to simpler representations of the material's stress–strain behavior, flaw shape and orientation, loading, and boundary conditions. If these assumptions are valid, one can perform fracture-mechanics evaluations without having to conduct any full-scale elastic–plastic finite element analysis. In addition, if the deformation theory of plasticity is valid, the J-integral can be split as

$$J = J_{\mathrm{e}} + J_{\mathrm{p}} \tag{6}$$

where J_{e} and J_{p} are the elastic and plastic components of J. For simple cracked structures, closed-form equations can be developed for J_{e} and J_{p}, and hence, J. The estimation methods for double-edged-notched tension (DENT) specimen (Fig. 2) and through-wall-cracked (TWC) pipe (Fig. 3) are briefly described in Appendices A and B.

2.3. J-based failure criteria

If J is a valid fracture parameter, there are several definitions of such failure criteria. Two definitions, commonly used in EPFM, are [13–16]: (1) initiation of crack growth and (2) unstable crack growth. They can be described by:

$$\text{Crack initiation} \quad J = J_{\mathrm{Ic}} \tag{7}$$

$$\text{Crack instability} \quad \begin{cases} J = J_R \\ \frac{\partial J}{\partial a} = \frac{\mathrm{d}J_R}{\mathrm{d}a} \end{cases} \tag{8}$$

The initiation of crack growth in a structure containing flaws can be characterized when the crack-driving force (J) exceeds the material fracture toughness (J_{Ic}). Eq. (7) represents this failure criterion. This is a good definition of failure when the uncracked ligament is small (e.g., part-through surface cracks in pipes or through-wall cracks in small-diameter pipes) or the amount of subsequent stable crack growth is limited (e.g., cracks in brittle materials). The initiation-based failure criterion is commonly used in piping and pressure vessel analysis [13–16].

In EPFM theory, the stable crack growth, if occurs in a structure, can also be characterized by the J-integral parameter with some limitations. In this regard, the J-tearing theory is a very prominent concept to quantify the stable crack growth. It is based on the fact that fracture instability can occur after some amount of stable crack growth in tough and ductile materials with an attendant higher applied load level at

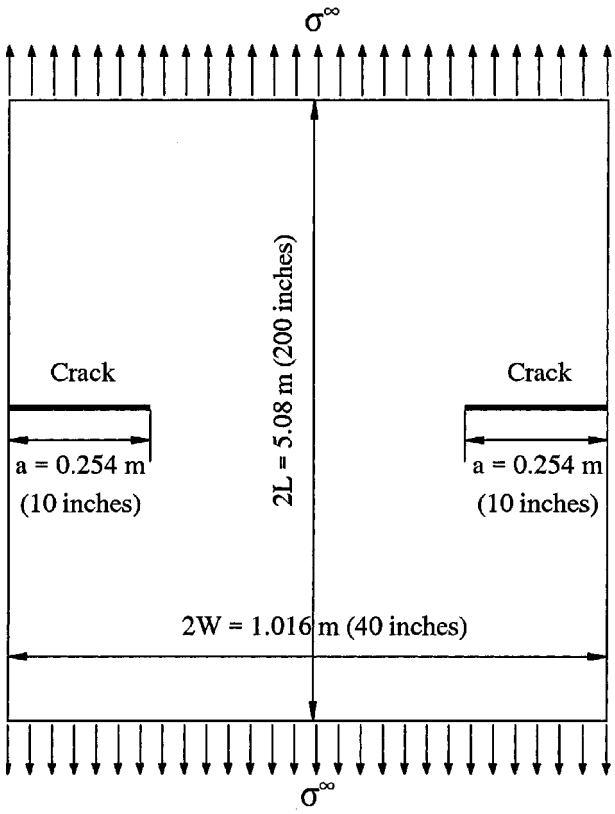

Fig. 2. A DENT specimen under far-field uniform tension.

fracture. The onset of fracture instability is defined when J and $\partial J/\partial a$ exceed J_R and $\mathrm{d}J_R/\mathrm{d}a$ simultaneously, as also expressed by Eq. (8). The corresponding crack-instability load is either equal to or higher than the crack-initiation load. The difference between these two failure loads can be significant, if the structural geometry and material permit appreciable amount of stable crack growth. Otherwise, the fracture criterion based on the initiation of crack growth provides a conservative estimate of structural integrity. This initiation-based criterion was used in the current probabilistic fracture analysis that will be presented in the forthcoming sections.

3. Probabilistic fracture mechanics and reliability

3.1. Random parameters and fracture response

Consider a cracked structure with uncertain mechanical and geometric characteristics that is subject to random loads. Denote by $\boldsymbol{X}$ an N-dimensional random vector with components $X_1, X_2, \ldots, X_N$ characterizing all uncertainty in the system and load parameters. Let J be a relevant crack-driving force that can be calculated from elastic–plastic finite element analysis. If J is a valid fracture parameter, then it can be applied to determine the failure probability of the cracked structure. Suppose that the structure fails when $J > J_{\mathrm{Ic}}$. This requirement cannot satisfied with certainty, because J depends on input vector $\boldsymbol{X}$ which is

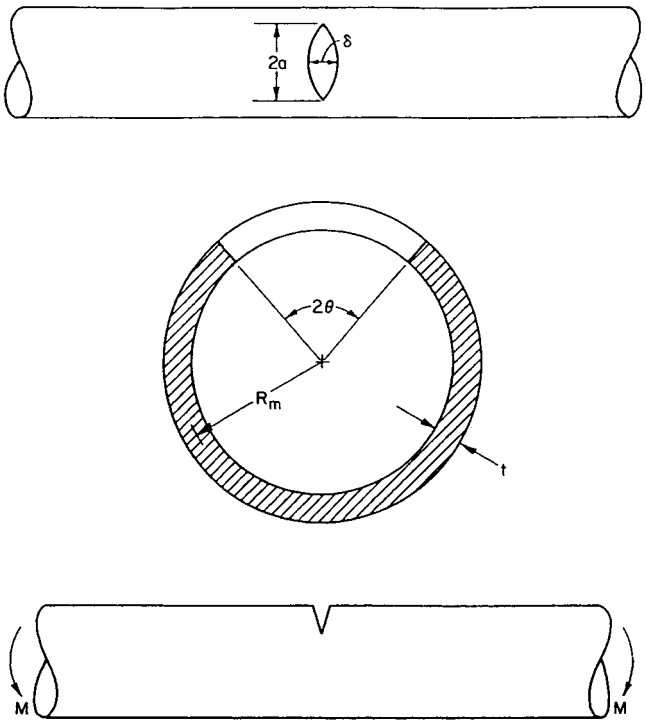

Fig. 3. A TWC pipe subjected to pure bending moment.

random and J_{Ic} itself is a random variable. Hence, the performance of the cracked structure should be evaluated by the reliability P_S or its complement, the probability of failure, P_F ($P_S = 1 - P_F$) defined as

$$P_F \stackrel{\text{def}}{=} \Pr[g(\boldsymbol{X}) < 0] \stackrel{\text{def}}{=} \int_{g(\boldsymbol{x})<0} f_{\boldsymbol{X}}(\boldsymbol{x})\mathrm{d}\boldsymbol{x} \tag{9}$$

where $f_{\boldsymbol{X}}(\boldsymbol{x})$ is the joint probability density function of $\boldsymbol{X}$, and $g(\boldsymbol{X})$ is the performance function given by

$$g(\boldsymbol{X}) = J_{Ic} - J. \tag{10}$$

Note that P_F in Eq. (9) represents the probability of initiation of crack growth which provides a conservative estimate of structural performance. A less conservative evaluation requires calculation of failure probability based on crack-instability criterion. The latter probability is more difficult to compute, since it must be obtained by incorporating crack-growth simulation in a nonlinear finite element analysis. However, if suitable approximations of J can be developed analytically (e.g., in J-estimation method), it can be easily calculated as well [2].

3.2. Reliability analysis by first- and second-order reliability methods

The generic expression for the failure probability in Eq. (9) involves multi-dimensional probability integration for its evaluation. In this study, standard reliability methods, such as FORM/SORM [20–28] were used to compute these probabilities. They are briefly described here to compute the probability of failure P_F in Eq. (9) assuming a generic N-dimensional random vector $\boldsymbol{X}$ and the performance function $g(\boldsymbol{x})$ defined by Eq. (10).

The FORM/SORM are based on linear (first-order) and quadratic (second-order) approximations of the limit state surface $g(\boldsymbol{x}) = 0$ tangent to the closest point of the surface to the origin of the space. The determination of this point involves nonlinear constrained optimization and is usually performed in the standard Gaussian image of the original space. The FORM/SORM algorithms involve several steps. First, the space $\boldsymbol{x}$ of uncertain parameters $\boldsymbol{X}$ is transformed into a new N-dimensional space $\boldsymbol{u}$ consisting of independent standard Gaussian variables $\boldsymbol{U}$. The original limit state $g(\boldsymbol{x}) = 0$ then becomes mapped into the new limit state $g_U(\boldsymbol{u}) = 0$ in the $\boldsymbol{u}$ space. Second, the point on the limit state $g_U(\boldsymbol{u}) = 0$ having the shortest distance to the origin of the $\boldsymbol{u}$ space is determined by using an appropriate nonlinear optimization algorithm. This point is referred to as the design point or beta point, and has a distance β_{HL} (known as reliability index) to the origin of the $\boldsymbol{u}$ space. Third, the limit state $g_U(\boldsymbol{u}) = 0$ is approximated by a surface tangent to it at the design point. Let such limit states be $g_{\mathrm{L}}(\boldsymbol{u}) = 0$ and $g_{\mathrm{Q}}(\boldsymbol{u}) = 0$, which correspond to approximating surfaces as hyperplane (linear or first-order) and hyperparaboloid (quadratic or second-order), respectively. The probability of failure P_{F} Eq. (9) is thus approximated by $\Pr[g_{\mathrm{L}}(\boldsymbol{U}) < 0]$ in FORM and $\Pr[g_{\mathrm{Q}}(\boldsymbol{U}) < 0]$ in SORM. These first-order and second-order estimates $P_{\mathrm{F},1}$ and $P_{\mathrm{F},2}$ are given by [20–28]

$$P_{\mathrm{F},1} = \Phi(-\beta_{\mathrm{HL}}) \tag{11}$$

$$P_{\mathrm{F},2} \cong \Phi(-\beta_{\mathrm{HL}}) \prod_{i=1}^{N-1} \left(1 - \kappa_i \frac{\phi(-\beta_{\mathrm{HL}})}{\Phi(-\beta_{\mathrm{HL}})}\right)^{-1/2} \tag{12}$$

where

$$\phi(u) = \frac{1}{\sqrt{2\pi}} \exp\left(-\frac{1}{2}u^2\right) \tag{13}$$

$$\Phi(u) = \frac{1}{\sqrt{2\pi}} \int_{-\infty}^{u} \exp\left(-\frac{1}{2}\xi^2\right) \mathrm{d}\xi \tag{14}$$

are the probability density and cumulative distribution functions, respectively, of a standard Gaussian random variable, and κ_i's are the principal curvatures of the limit state surface at the design point. Further details of FORM/SORM equations are available elsewhere [20–28].

FORM/SORM are standard computational methods of structural reliability theory. In this study, a modified HL–RF algorithm, described in Appendix C, was used to solve the associated optimization problem. The first- and second-order sensitivities were calculated numerically by the finite difference method.

4. Computer programs probabilistic fracture code and probabilistic leak-before-break analysis

Two computer codes titled *pro*babilistic *frac*ture *c*ode (PROFRAC) and *pro*babilistic *l*eak-*b*efore-*b*reak analysis (PROLBB) were developed/refined to calculate the probability of failure of cracked structures. These codes provide a computational framework for performing probabilistic fracture-mechanics analysis based on J-integral evaluations of two- and three-dimensional cracked structures subject to quasi-static loads. PROFRAC is a FEM-based code, whereas PROLBB is a J-estimation-based code. Further details are given below.

The PROFRAC program [8] involves (1) EPFM analysis by the nonlinear FEM, (2) statistical models of uncertainty for random loads, crack size, and material properties, and (3) standard methods of structural reliability theory. PROFRAC has been enhanced to interface with several commercial finite-element codes

including ABAQUS (version 5.6) [29]. In PROFRAC, one can model the relevant parameters in the input deck of ABAQUS as random variables. Both LEFM- and EPFM-based fracture theories are supported by PROFRAC. A number of finite element types can be chosen for probabilistic finite element analysis. The probabilistic analysis is completely automated. However, the current version of PROFRAC can only calculate probability of failure based on initiation of crack growth. The calculation of failure probability based on the instability of crack growth is more complicated and is beyond the current capability of PROFRAC. Also, the random crack size can be modeled only for two-dimensional problems. Work is currently underway to incorporate fracture instability in the performance criteria and extend statistical models to include random crack geometry for three-dimensional structures.

The PROLBB program [6] involves (1) EPFM analysis by the J-estimation methods, (2) statistical models of uncertainty for random loads, crack size, and material properties, and (3) standard computational methods of structural reliability theory. PROLBB, which was originally developed in the Short Cracks in Piping and Piping Welds Program [9], has been extended to include the GE/EPRI equations for J-integral analysis [2]. Using PROLBB, one can model any parameters of GE/EPRI equations as random variables. It can calculate probability of failure based on both initiation and instability of ductile crack growth.

5. Numerical examples

In this paper, two numerical examples based on a two- and a three-dimensional structures are presented. A major objective was to examine if the probabilistic analysis by J-estimation method (PROLBB) is adequate when compared with that by FEM (PROFRAC). As mentioned before, the performance function for the failure criterion is based on the initiation of crack growth only.

5.1. Example 1: a double-edged-notched tension specimen

Consider a DENT specimen (Fig. 2) with width, $2W = 1.016$ m (40 in.), length, $2L = 5.08$ m (200 in.), and crack length, $a = 0.254$ m (10 in.). The specimen material is TP304 stainless steel and the operating temperature is 288°C (550°F). It was assumed that both load and material properties are random. Table 1 shows the means, coefficients of variation (COV), and probability distributions of these random parameters. Most of these values came from statistical characterization of actual material property data [6]. The random variables were assumed to be statistically independent. The deterministic material parameters involved: reference stress, $\sigma_0 = 154.78$ MPa (22,450 psi) and Poisson's ratio, $v = 0.3$.

Fig. 4(a) shows a finite element mesh for 1/4 model due to the symmetry of this problem. A total of 114 elements and 393 nodes were used in this mesh. Second-order elements from ABAQUS element library were

Table 1
Statistical properties of random input for DENT specimen

Random variable	Mean	COV[a]	Probability distribution	Reference
Elastic modulus (E)	206.8 GPa	0.05	Gaussian	–[b]
Ramberg–Osgood coefficient (α)	8.073	0.439	Lognormal	[6]
Ramberg–Osgood exponent (n)	3.8	0.146	Lognormal	[6]
Initiation fracture toughness (J_{Ic})	1242.6 kJ/m^2	0.47	Lognormal	[6]
Far-field tensile stress (σ^{∞})	Variable[c]	0.1	Gaussian	–[b]

[a] COV = standard deviation/mean.
[b] Arbitrarily assumed.
[c] Varies from 48.3 to 103.4 MPa (7000–15,000 psi).

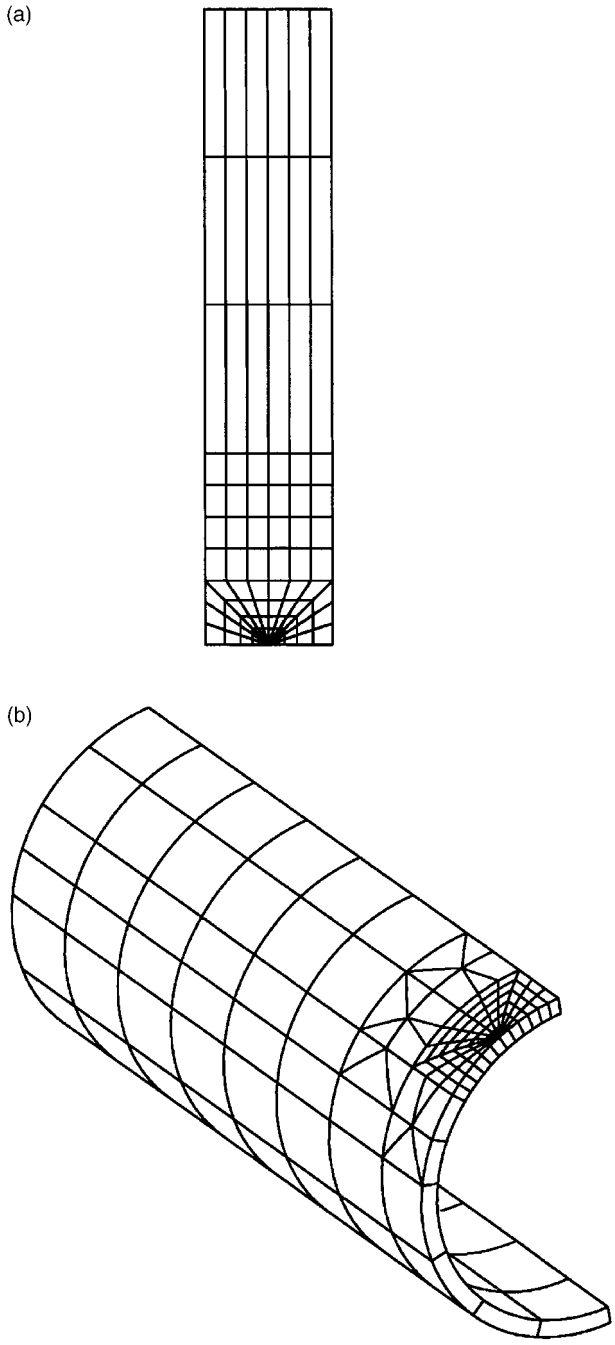

Fig. 4. Finite element meshes for DENT and TWC pipe: (a) a DENT specimen (1/4 model) and (b) a TWC pipe specimen (1/4 model).

used. Both plane stress and plane strain conditions were studied. For plane stress, the element type was CPS8R – the reduced integration, eight-noded quadrilateral element. For plane strain, the element type CPE8RH was used. This element is a mixed formulation element and is typically used to handle the in-

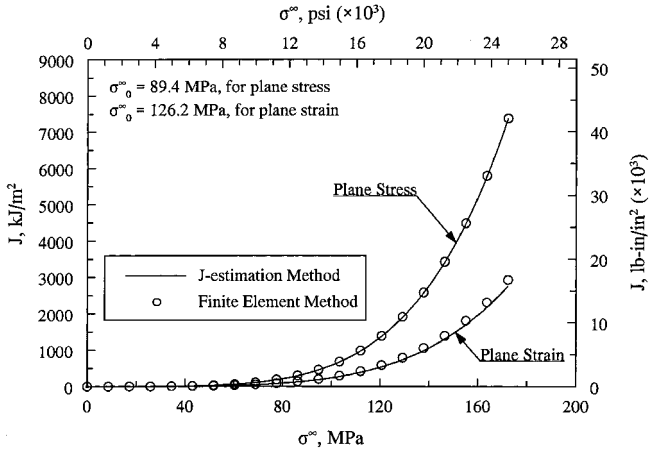

Fig. 5. Predicted J-integral for DENT specimen by J-estimation and FEMs.

compressibility constraint for plane strain. Focused elements were used in the vicinity of crack tip. The material model was the deformation theory, Ramberg–Osgood model defined by Eq. (1).

Fig. 5 shows the deterministic finite element results of J from the PROFRAC (ABAQUS) code as a function of σ^{∞} for plane stress and plane strain conditions. The mean values of material properties, defined in Table 1, were used to generate the plots of Fig. 5. Also plotted in the same figure are the corresponding solutions by the J-estimation method (i.e., Eqs. (A.1)–(A.5)) in the PROLBB code. The results from J-estimation method match very well with the finite element solutions for the load intensities and material constants considered. In both methods, the crack driving force (J) is higher for plane stress than that for plane strain as expected.

Following deterministic comparisons of J, several probabilistic analyses were performed by PROFRAC to calculate probability of failure, [2] P_F, as a function of mean far-field tensile stress, $E[\sigma^{\infty}]$, where $E[\cdot]$ is the expectation (mean) operator. Fig. 6 shows such results in the form of P_F vs. $E[\sigma^{\infty}]$ plots for both plane stress and plane strain conditions. The probability of failure was calculated by SORM (i.e., Eq. (12)), which was validated by Monte Carlo with importance sampling in a previous study [8]. The failure probability increases with the mean stress intensity as expected. Due to higher demand of J (see Fig. 5), the probability of failure in plane stress is generally larger than that in plane strain regardless of the load intensity. Also plotted in the same figure, are the corresponding probability estimates by PROLBB. It appears that the J-estimation method can provide accurate estimates of failure probability when compared with generally more accurate finite element analysis. The probabilistic analysis by PROLBB was also performed using SORM.

The failure probabilities in Fig. 6 are valid for a deterministic crack size only. To evaluate the effects of uncertainty in crack size, the following additional *elastic* analyses were performed. They involved modeling normalized crack length, a/W, as a lognormal random variable with mean, $\mu_{a/W} = 0.5$ (keeping $W = 0.508$ m as deterministic) and coefficient of variation, $v_{a/W} = 0\%$, 10%, 20%, and 40%. Using the J-estimation method (PROLBB), Fig. 7(a) and (b) show the plots of P_F vs. $E[\sigma^{\infty}]$ for plane stress and plane strain conditions, respectively, for both deterministic ($v_{a/W} = 0$) and random ($v_{a/W} = 10\%$, 20%, and 40%) crack sizes. The results indicate that the failure probability increases with the COV (uncertainty) of a/W as

[2] The failure probability in this paper refers to probability of fracture initiation (see Eq. (9)).

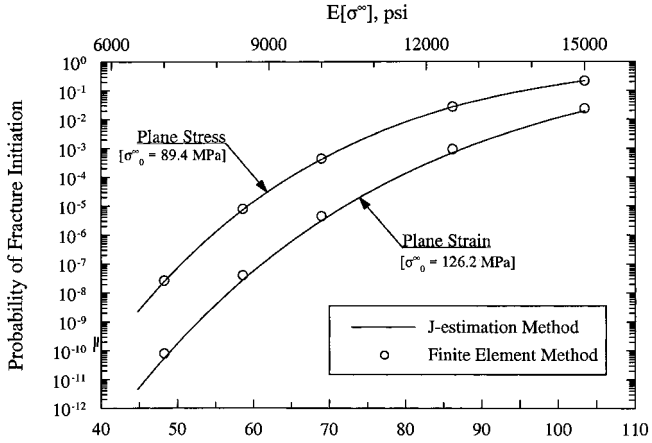

Fig. 6. Probability of failure for DENT specimen by *J*-estimation and FEMs.

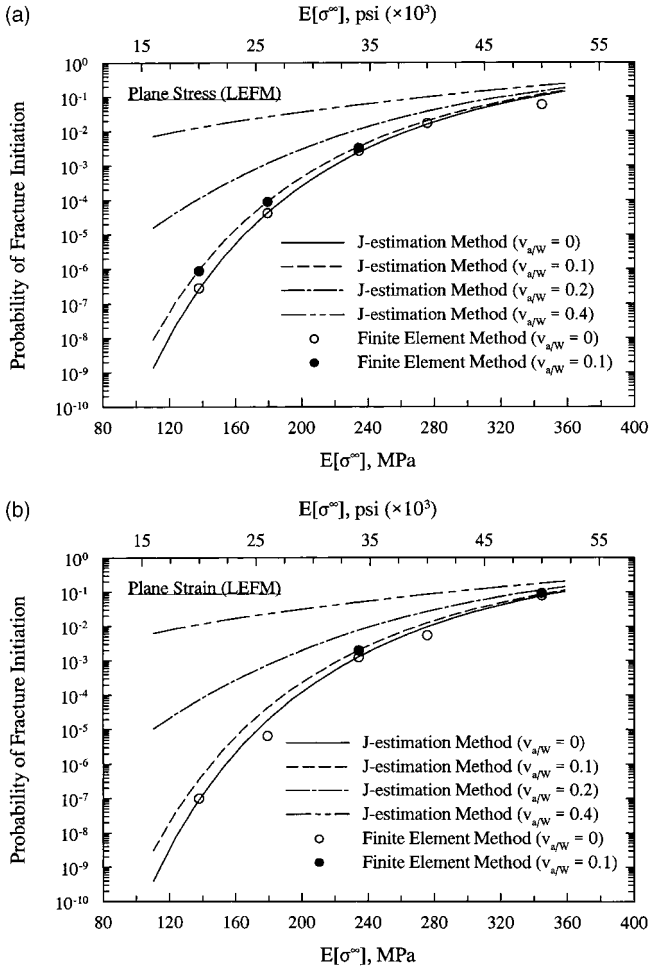

Fig. 7. Probability of failure for DENT specimen for random crack size (elastic analysis): (a) plane stress and (b) plane strain.

expected and can be much larger than the probabilities calculated for a deterministic crack size, particularly when the uncertainty in a/W is large.

Also included in Fig. 7(a) and (b) are a few results of FEM-based probabilistic analysis (PROFRAC) when $v_{a/W} = 0\%$ and 10%. The agreement between the FEM and J-estimation method is excellent. Work is currently undergoing to predict these failure probabilities from elastic–plastic analysis involving random crack size.

5.2. Example 2: a through-wall-cracked pipe specimen

Consider a TWC pipe (Fig. 3) subjected to remote bending moment, M. The pipe has mean radius, $R_m = 355.6$ mm (14 in.), wall thickness, $t = 35.6$ mm (1.4 in.), and normalized crack angle, $\theta/\pi = 0.125$. The pipe material is TP304 stainless steel with the temperature of 288°C (550°F). Table 2 shows the means, coefficients of variation, and probability distributions of tensile parameters (E, α, n), fracture toughness parameter (J_{Ic}), and bending moment (M). As mentioned before, the statistics of material properties were obtained from actual TP304 stainless steel data at 288°C (550°F) [6]. However, the probabilistic characteristics of M were chosen arbitrarily. For this example, $\sigma_0 = 154.78$ MPa (22,450 psi) and $v = 0.3$.

A finite element mesh for the TWC pipe specimen is shown in Fig. 4(b). A quarter model was used to take advantage of the symmetry. 20-Noded isoparametric solid elements (C3D20R) from the ABAQUS library were used with focused elements at the crack tip. A total of 150 elements and 1098 nodes was used. The stress–strain curve was model by Ramberg–Osgood equation (see Eq. (1)) in this example as well.

Fig. 8 shows the plots of P_F vs. $E[M]$ obtained by FEM and J-estimation models using PROFRAC and PROLBB, respectively. In both analyses, the reliability analyses were performed by SORM and assuming a deterministic crack size. The two sets of results from these analyses match extremely well. Once again, it shows that a probabilistic analysis based on J-estimation model can provide excellent measures of failure probability.

Fig. 9 shows the similar plots of failure probabilities by J-estimation method for random crack sizes. It was assumed that the normalized crack angle, θ/π has mean, $\mu_{\theta/\pi} = 0.125$ and coefficient of variation, $v_{\theta/\pi} = 0\%$, 10%, 20%, and 40%, and follows the lognormal distribution. From Fig. 9, the uncertainty in crack size appear to have a significant effect on increasing the failure probability, particularly when the $v_{\theta/\pi}$ is large. A similar observation was made when analyzing the DENT specimen.

Note, the probabilistic calculations for random crack size in TWC pipes could not be made by the present FEM-based probabilistic model. This is because, for three-dimensional cracked structures, modeling automatic crack-tip mesh as a function of random crack size is beyond the current capability of PROFRAC. Work is currently underway to include random crack size in PROFRAC.

Table 2
Statistical properties of random input for TWC pipe specimen

Random variable	Mean	COV[a]	Probability distribution	Reference
Elastic modulus (E)	182.7 GPa	0.05	Gaussian	–[b]
Ramberg–Osgood coefficient (α)	8.073	0.439	Lognormal	[6]
Ramberg–Osgood exponent (n)	3.8	0.146	Lognormal	[6]
Initiation fracture toughness (J_{Ic})	1242.6 kJ/m^2	0.47	Lognormal	[6]
Bending moment (M)	Variable[c]	0.1	Gaussian	–[b]

[a] COV = standard deviation/mean.
[b] Arbitrarily assumed.
[c] Varies from 1130 to 2260 kN m (10×10^6–20×10^6 lb in.).

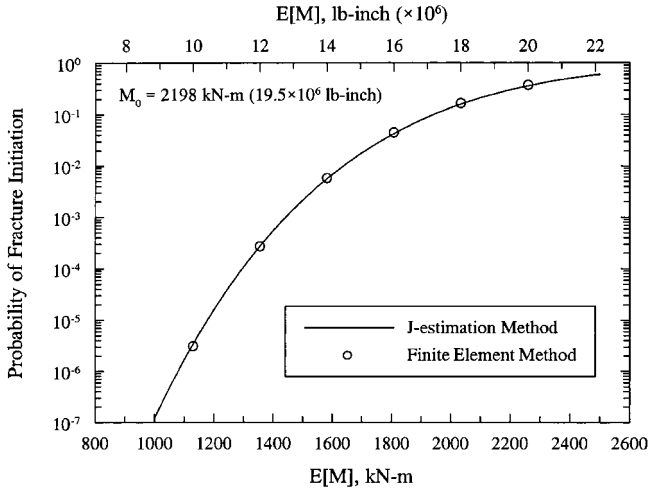

Fig. 8. Probability of failure for TWC pipe by *J*-estimation and FEMs (deterministic crack size).

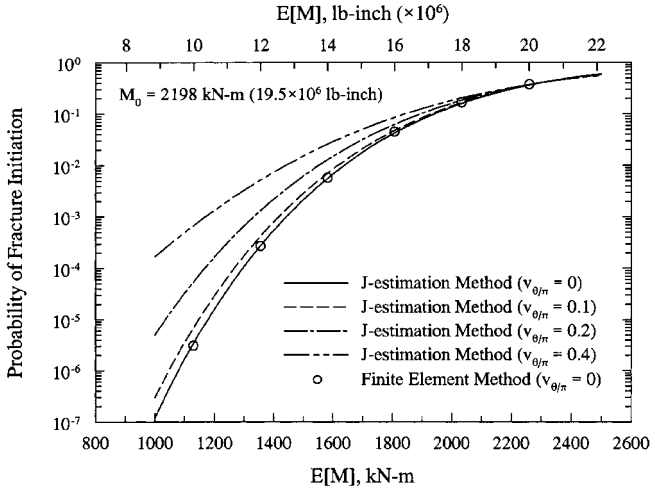

Fig. 9. Probability of failure for TWC pipe by *J*-estimation and FEMs (random crack size).

6. Summary and conclusions

A newly developed probabilistic model based on elastic–plastic finite element analysis was applied to evaluate the adequacy of *J*-estimation models commonly used for fracture-mechanics analysis of ductile cracked structures. In both models, the analyses involve (1) EPFM, (2) statistical models of loads, crack size, and material properties and (3) standard computational reliability methods. Numerical examples are presented to compare the failure probability estimates for a two-dimensional DENT specimen and a three-dimensional TWC pipe specimen. The results show that:

- *J*-estimation analysis using Ramberg–Osgood model of stress–strain curve provides accurate estimates of failure probability when compared with those predicted by generally more accurate finite element analysis;

- The uncertainty in the crack size, if exists, can have a significant effect on increasing the probability of failure, particularly when the crack size has a large COV; and
- A finite EPFM model is useful in benchmarking approximate results of *J*-estimation analysis. However, more work is needed to enhance its current capabilities, e.g., by generating automatic crack-tip mesh as a function of random crack size and by modeling automatic crack-growth simulation for predicting probability of crack-growth instability. These are subjects of current research by the author.

Acknowledgements

The work presented in this paper was supported by the Faculty Early Career Development Program of the US National Science Foundation (grant no. CMS-9733058). The program directors were Drs. Ken Chong and Sunil Saigal.

Appendix A. *J*-estimation for DENT and TWC pipe specimens

A.1. A double-edged-notched tension specimen

Consider a DENT specimen subjected to quasi-static far-field tension stress, σ^{∞}. The geometry of the DENT specimen, shown in Fig. 2, has width, $2W$, length, $2L$, thickness, B, and crack length, a. The equations for J_e and J_p are given below.

Elastic solution [30]

$$J_e = \frac{K_I^2}{E'} \tag{A.1}$$

where

$$K_I = \sigma^{\infty}\sqrt{\pi a}\left[1.12 + 0.2(a/W) - 1.2(a/W)^2 + 1.93(a/W)^3\right] \tag{A.2}$$

is the mode-I stress-intensity factor,

$$E' = \begin{cases} E, & \text{plane stress} \\ \frac{E}{1-\nu^2}, & \text{plane strain} \end{cases} \tag{A.3}$$

is the effective modulus of elasticity, and ν is the Poisson's ratio.

Plastic solution [30]

$$J_p = \frac{\alpha\sigma_0^2}{E}(W-a)h_1(a/W,n)\left(\frac{P}{P_0}\right)^{n+1} \tag{A.4}$$

where $P = 2WB\sigma^{\infty}$ is the far-field tensile load,

$$P_0 = \begin{cases} \frac{4}{\sqrt{3}}\sigma_0(W-a)B, & \text{plane stress} \\ \left[0.72 + 1.82\left(1-\frac{a}{W}\right)\right]\sigma_0 WB, & \text{plane strain} \end{cases} \tag{A.5}$$

is the reference load, and $h_1(a/W,n)$ is a dimensionless plastic influence function that depends on crack geometry and material hardening exponent. The values of $h_1(a/W,n)$ are tabulated in Ref. [30].

A.2. A through-wall-cracked pipe specimen

Consider a TWC pipe under pure bending moment, M. As shown in Fig. 3, the pipe has mean radius, R_m, wall thickness, t, and a symmetrically centered through-wall crack with mean length, $2a = 2R_m\theta$, where 2θ is the total crack angle. The equations for J_e and J_p are given in the following subsections.

Elastic solution [2,31]

$$J_e = \frac{\theta}{\pi} F(\theta/\pi, R_m/t)^2 \frac{M^2}{ER_m^3 t^2} \tag{A.6}$$

where $F(\theta/\pi, R_m/t)$ is a dimensionless elastic influence function that depends on pipe and crack geometry. According to Rahman [2],

$$F(\theta/\pi, R_m/t) = 1 + \{A_1 \quad A_2 \quad A_3\} \begin{Bmatrix} (\theta/\pi)^{1.5} \\ (\theta/\pi)^{2.5} \\ (\theta/\pi)^{3.5} \end{Bmatrix} \{B_1 \quad B_2 \quad B_3 \quad B_4\} \begin{Bmatrix} 1 \\ (R_m/t) \\ (R_m/t)^2 \\ (R_m/t)^3 \end{Bmatrix} \tag{A.7}$$

where A_i ($i = 1$–3) and B_i ($i = 1$–4) are constant coefficients which can be calculated from best fit of finite element results [2]. The values of these coefficients are given in Appendix B.

Plastic solution [2,31]

$$J_p = \frac{\alpha\sigma_0^2}{E} R_m \theta \left(1 - \frac{\theta}{\pi}\right) h_1(\theta/\pi, n, R_m/t) \left(\frac{M}{M_0}\right)^{n+1} \tag{A.8}$$

where

$$M_0 = 4\sigma_0 R_m^2 t \left[\cos\frac{\theta}{2} - \frac{1}{2}\sin\theta\right] \tag{A.9}$$

is the reference moment, and $h_1(\theta/\pi, n, R_m/t)$ is a dimensionless plastic influence function that depends on pipe geometry, crack geometry, and material hardening exponent. According to Rahman [2],

$$h_1(\theta/\pi, n, R_m/t) = \{1 \quad (\theta/\pi) \quad (\theta/\pi)^2 \quad (\theta/\pi)^3\} \begin{bmatrix} C_{00} & C_{10} & C_{20} & C_{30} \\ C_{01} & C_{11} & C_{21} & C_{31} \\ C_{02} & C_{12} & C_{22} & C_{32} \\ C_{03} & C_{13} & C_{23} & C_{33} \end{bmatrix} \begin{Bmatrix} 1 \\ n \\ n^2 \\ n^3 \end{Bmatrix} \tag{A.10}$$

where C_{ij} ($i, j = 0$–3) are coefficients that depend on R_m/t and can also be calculated from best fit of finite element results [2]. The values of these coefficients are given in Appendix B.

Eqs. (A.1)–(A.10) represent the well-known GE/EPRI method [30,31]. It is one of many J-estimation methods currently available for analyzing cracked structures [16]. Due to limited scope, all J-estimation analyses in this study were based on the GE/EPRI method alone.

Appendix B. Coefficients A_i, B_i, and C_{ij}

B.1. Coefficients A_i and B_i

Let $\boldsymbol{A} = \{A_1 \quad A_2 \quad A_3\}^T$ and $\boldsymbol{B} = \{B_1 \quad B_2 \quad B_3 \quad B_4\}^T$ be two real vectors with the coefficients, A_i and B_i as their components, respectively. According to Rahman [2],

$$\boldsymbol{A} = \{0.006215 \quad 0.013304 \quad -0.01838\}^T \tag{B.1}$$

$$\boldsymbol{B} = \{\, 175.577 \quad 91.69105 \quad -5.53806 \quad 0.15116 \,\}^{\mathrm{T}}. \tag{B.2}$$

B.2. Coefficients C_{ij}

Let $\boldsymbol{C} = \left[C_{ij}\right]$, $i, j = 0$–3, be a real matrix with the coefficients, C_{ij} as its components. According to Rahman [2],

$$\boldsymbol{C} = \begin{bmatrix} 3.74009 & 1.43304 & -0.10216 & 0.0023 \\ -0.19759 & -10.19727 & -0.45312 & 0.04989 \\ 36.42507 & 17.03413 & 3.36981 & -0.21056 \\ -70.4846 & -14.69269 & -2.90231 & 0.15165 \end{bmatrix} \tag{B.3}$$

For $R_{\mathrm{m}}/t = 10$,

$$\boldsymbol{C} = \begin{bmatrix} 3.39797 & 1.31474 & -0.07898 & 0.00287 \\ -3.07265 & 4.34242 & -2.48397 & 0.11476 \\ 131.7381 & -79.02833 & 16.18829 & -0.66912 \\ -234.6221 & 117.0509 & -20.30173 & 0.79506 \end{bmatrix} \tag{B.4}$$

For $R_{\mathrm{m}}/t = 20$,

$$\boldsymbol{C} = \begin{bmatrix} 4.07828 & -1.55095 & 0.67206 & -0.0442 \\ -18.21195 & 69.92277 & -18.41884 & 1.11308 \\ 357.4929 & -453.1582 & 108.0204 & -6.56651 \\ -602.7576 & 617.9074 & -144.9435 & 8.9022 \end{bmatrix}. \tag{B.5}$$

See Ref. [2] for explanation on how these coefficients were calculated from extensive elastic–plastic finite element analyses.

Appendix C. A modified HL–RF method

In FORM/SORM, the main effort is calculating the reliability index, $\beta_{\mathrm{HL}} = \|\boldsymbol{u}^*\|$ by finding the design point, $\boldsymbol{u}^*$, which can be formulated as a constrained optimization problem defined by

$$\min_{\boldsymbol{u}\in\Re^N} \|\boldsymbol{u}\| \quad \text{s.t. } g_U(\boldsymbol{u}) = 0 \tag{C.1}$$

where $\Re^N$ is an N-dimensional real vector space, $\boldsymbol{u} \in \Re^N$ is the space of standard Gaussian vector, $\boldsymbol{U} \in \Re^N$, and $g_U(\boldsymbol{u}) : \Re^N \mapsto \Re$ is the transformed performance function in $\boldsymbol{u}$-space, and

$$\|\boldsymbol{u}\| \stackrel{\mathrm{def}}{=} \sqrt{\sum_{i=i}^{N} u_i^2} \tag{C.2}$$

is the Euclidean $\mathscr{L}_2$-norm of the N-dimensional vector, $\boldsymbol{u}$. A modified HL–RF method, originally proposed by Hasofer and Lind [20] and later extended by Rackwitz and Fiessler [22] and modified by Liu and Kiureghian [32], is one of the most widely used and robust optimization methods to solve the reliability problem in Eq. (C.1) [21,32]. The original HL–RF method involves an iterative algorithm given by the following recursive formula:

$$\boldsymbol{u}^{k+1} = \frac{1}{\|\nabla g_U(\boldsymbol{u}^k)\|^2}\left[\nabla g_U(\boldsymbol{u}^k)^{\mathrm{T}}\boldsymbol{u}^k - g_U(\boldsymbol{u}^k)\right]\nabla g_U(\boldsymbol{u}) \tag{C.3}$$

where, $\boldsymbol{u}^k$ is the vector at kth iteration, $\nabla = \{\partial/\partial u_1, \partial/\partial u_2, \ldots, \partial/\partial u_N\}^{\mathrm{T}}$ is a vector of gradient operators, and $\nabla g_U(\boldsymbol{u}^k)$ is the gradient of scalar field, $g_U(\boldsymbol{u}^k)$. The algorithm proceeds iteratively until convergence is achieved, i.e., when

$$\left|u_i^{k+1} - u_i^k\right| \leqslant \varepsilon_{\mathrm{con}}, \quad \text{for all } i \tag{C.4}$$

and

$$|g_U(\boldsymbol{u}^*)| \cong \left|g_U(\boldsymbol{u}^{k+1})\right| \leqslant \varepsilon_{\mathrm{con}} \tag{C.5}$$

where $\varepsilon_{\mathrm{con}}$ is a small control parameter assigned by the user. From the past experience of authors, a value of $\varepsilon_{\mathrm{con}} = 10^{-4}$–$10^{-3}$ usually yields satisfactory estimates of β_{HL}.

To improve the robustness of Eq. (C.3), Liu and Kiureghian proposed a non-negative merit function, $m(\boldsymbol{u}^k)$, which is defined as [32]

$$m(\boldsymbol{u}^k) = \frac{1}{2}\left\|\boldsymbol{u}^k - \frac{\nabla g_U(\boldsymbol{u}^k)^{\mathrm{T}}\boldsymbol{u}^k}{\|\nabla g_U(\boldsymbol{u}^k)\|^2}\nabla g_U(\boldsymbol{u}^k)\right\|^2 + \frac{1}{2}c g_U(\boldsymbol{u}^k)^2 \tag{C.6}$$

where, c is some scalar positive constant. The merit function in Eq. (C.6) is a convenient guide for selecting step size, since it is a function of quantities already known at the current iteration point, $\boldsymbol{u}^k$. This modification greatly improves the convergence (although not strictly guaranteed) of the original HL–RF method [32].

References

[1] Provan JW. Probabilistic fracture mechanics and reliability. Dordrecht, The Netherlands: Martinus Nijhoff Publishers; 1987.
[2] Rahman S. A stochastic model for elastic–plastic fracture analysis of circumferential through-wall-cracked pipes subject to bending. Engng Fract Mech 1995;52:2.
[3] Warke RW, Wang YY, Ferregut CF, Carrasco CJ, Horsley DJ. A FAD-based method for probabilistic flaw assessment of strength-mismatched girth welds. Proceedings of the 1999 ASME Pressure Vessel and Piping Conference, Boston, MA, 1999.
[4] Wilson R, Bernard JM, Ainsworth RA. Relationship between conditional failure probabilities and corresponding reserve factors derived from the R6 failure assessment diagram. Proceedings of the 1996 ASME Pressure Vessel and Piping Conference, Montreal, Canada, 1996.
[5] Heinfling G, Pendola M, Hornet P. Reliability level provided by safety factors in defect assessment procedures. Proceedings of the 1999 ASME Pressure Vessel and Piping Conference, Boston, MA, 1999.
[6] Rahman S, Ghadiali N, Paul D, Wilkowski G. Probabilistic pipe fracture evaluations for leak-rate-detection applications. NUREG/CR-6004, US Nuclear Regulatory Commission, Washington, DC, 1995.
[7] Hornet P, Pendola M, Lemaire M. Failure probability calculation of an axisymmetrically cracked pipe under pressure and tension using a finite element code. Proceedings of the 1998 ASME Pressure Vessel and Piping Conference, San Diego, CA, 1998.
[8] Rahman S, Kim JS. Probabilistic fracture mechanics for nonlinear structures. Proceedings of seventh International Conference on Structural Safety and Reliability, Kyoto, Japan, November 1997; Also, submitted to International Journal of Pressure Vessels and Piping, 2000.
[9] Wilkowski GM, et al. Short cracks in piping and piping welds program. NUREG/CR-4599, US Nuclear Regulatory Commission, vol. 1–3, nos. 1–2, Washington, DC, 1991–1994.
[10] Rice JR. A path independent integral and the approximate analysis of strain concentration by notches and cracks. J Appl Mech 1968;35:379–86.
[11] Hutchinson JW. Fundamentals of the phenomenological theory of nonlinear fracture mechanics. J Appl Mech 1983;50:1042–51.
[12] Rice JR, Rosengren GF. Plane strain deformations near a crack tip in a power-law hardening material. J Mech Phys Solids 1968;16:1–12.
[13] Wilkowski GM. Degraded piping program – phase II. Final and Semiannual Reports, NUREG/CR-4082, vols. 1–8, US Nuclear Regulatory Commission, Washington, DC, 1985–1989.
[14] Schmidt RA, Wilkowski GW, Mayfield M. The international piping integrity research group (IPIRG) program – an overview. Proceedings of 11th International Conference on Structural Mechanics in Reactor Technology, Paper G23/1, Tokyo, Japan, 1991.

[15] Hopper A, Mayfield M, Olson R, Scott P, Wilkowski G. Overview of the IPIRG-2 program – seismic loaded cracked pipe system experiments. Proceedings of 13th International Conference on Structural Mechanics in Reactor Technology, Division F, paper F12-1, 1995.
[16] Rahman S, Wilkowski G, Brust F. Fracture analysis of full-scale pipe experiments on stainless steel flux welds. Nucl Engng Des 1996;160:77–96.
[17] Shih CF, Moran B, Nakamura T. Energy release rate along a three-dimensional crack front in a thermally stressed body. Inter J Frac 1968;30:79–102.
[18] Moran B, Shih CF. A general treatment of crack tip contour integrals. Inter J Fract 1987;35:295–310.
[19] Anderson TL. Fracture mechanics: fundamentals and applications. 2nd ed. Boca Raton, FL: CRC Press; 1995.
[20] Hasofer AM, Lind NC. An exact and invariant first-order reliability format. J Engng Mech 1974;100:111–21.
[21] Madsen HO, Krenk S, Lind NC. Methods of structural safety. Englewood Cliffs, NJ: Prentice-Hall; 1986.
[22] Rackwitz R, Fiessler B. Structural reliability under combined random load sequence. Comput Struct 1978;9:489–94.
[23] Fiessler B, Nuemann HJ, Rackwitz R. Quadratic limit states in structural reliability. J Engng Mech 1979;105(4):661–76.
[24] Breitung K. Asymptotic approximations for multinormal integrals. J Engng Mech 1984;110(3):357–66.
[25] Hohenbichler M, Gollwitzer S, Kruse W, Rackwitz R. New light on first- and second-order reliability methods. Struct Safety 1987;4:267–84.
[26] Tvedt L. Distribution of quadratic forms in normal space – application to structural reliability. J Engng Mech 1990;116(6): 1183–97.
[27] Der Kiureghian A, Lin HZ, Hwang SF. Second-order reliability approximations. J Engng Mech 1987;113(8):1208–25.
[28] Der Kiureghian A, Liu P-L. Structural reliability under incomplete probability information. J Engng Mech 1986;112(1):85–104.
[29] ABAQUS. User's guide and theoretical manual. Version 5.6, Hibbitt, Pawtucket, RI: Karlsson and Sorenson; 1997.
[30] Kumar V, German MD, Shih CF. An engineering approach for elastic–plastic fracture analysis. EPRI NP-1931, Electric Power Research Institute, Palo Alto, CA, 1981.
[31] Kumar V, German MD, Wilkening WW, Andrews WR, deLorenzi HG, Mowbray DF. Advances in elastic–plastic fracture analysis. EPRI NP-3607, Electric Power Research Institute, Palo Alto, CA, 1984.
[32] Liu PL, Kiureghian AD. Optimization algorithms for structural reliability. Struct Safety 1991;9:161–77.